COMMUNICATION

ChemComm
www.rsc.org/chemcomm

Parallel synthesis and characterization of photoelectrochemically and electrochromically active tungsten–molybdenum oxides

Sung-Hyeon Baeck,[a] Thomas F. Jaramillo,[a] Dae Hong Jeong[b] and Eric W. McFarland*[a]

[a] *Department of Chemical Engineering, University of California, Santa Barbara, California 93106-5080, USA. E-mail: mcfar@engineering.ucsb.edu; Fax: 1-805-893-4731; Tel: 1-805-893-4343*

[b] *Department of Chemistry Education, Seoul National University, San56-1, Shillim-Dong, Kwanak-Ku, Seoul, Korea*

Received (in Cambridge, UK) 3rd November 2003, Accepted 16th December 2003
First published as an Advance Article on the web 19th January 2004

Single phase tungsten–molybdenum mixed oxide films ($W_{1-x}Mo_xO_3$) were successfully synthesized by automated parallel electrodeposition, and distinct structural changes were observed as a function of composition. A monoclinic structure (β-phase) was observed in mixed oxides with less than 90% Mo, and above 90% Mo, orthorhombic structure (α-phase) was identified.

Tungsten oxide (WO_3) and molybdenum oxide (MoO_3) are indirect bandgap semiconductors with interesting photoelectrochemical properties. They are presently used in electrochromic devices and chemical sensors and show promise as low cost materials for solar energy applications.[1–3] Tungsten–molybdenum mixed oxides ($W_{1-x}Mo_xO_3$) have been of interest because of improved electrochromic performance. Tungsten–molybdenum mixed oxides have been prepared by high temperature calcination of a powder mixture of tungsten oxide and molybdenum oxide,[4] thermal co-evaporation of WO_3 and MoO_3,[5] and chemical vapor deposition.[6,7] There have been several reports of electrodeposition of tungsten–molybdenum mixed metal oxides,[8,9] however, there was minimal structural analysis and no evidence for or against phase separation. In this communication, we apply automated parallel chemistry for the electrodeposition of the first reported atomically mixed tungsten–molybdenum oxides ($W_{1-x}Mo_xO_3$, x = 0.0, 0.05, 0.1, 0.2, 0.3, 0.5, 0.7, 0.8, 0.9 0.95, 1.0) and their detailed structural and functional analysis.

The electrolyte was prepared by first grinding mixtures of tungsten and molybdenum metal powders in a porcelain mortar and pestle. The mixed metal powder was then dissolved in 60 ml of 30% hydrogen peroxide solution. Excess hydrogen peroxide was subsequently decomposed with platinum black. A 50:50 water and isopropanol mixture was used to dilute each solution to a total metal (W + Mo) concentration of 50 mM and the concentration of molybdenum *vs*. tungsten was varied from 0 to 100 mol% for each electrolyte. Library synthesis (5 × 9 arrays) was performed in a parallel electrochemical reactor on ITO-coated glass substrates which had been cleaned with aqueous detergent, acetone and isopropanol. The cathodic-potentiostatic deposition was performed in a parallel electrochemical cell array.[10] In brief, the assembly consisted of a 1 inch thick polypropylene block with 1/4 inch diameter holes. Using independent o-rings for sealing, the block was affixed to the ITO substrate, forming 45 isolated working electrodes. An array of 45 stainless steel pins was inserted into the polypropylene wells and used as a counter electrode, forming 45 individual two-electrode cells. Diversity in composition was achieved by variations of W:Mo ratios in the metal mixture. All films were deposited for 10 minutes at −1.8 V vs the stainless steel counter electrodes. This potential correlates to −0.4 V *vs*. SCE in a 50 mM metal–peroxo electrolyte.

The film compositions were analyzed by energy dispersive spectroscopy (EDS) and correlated remarkably well to electrolyte compositions within the error range of ±5% (data not shown). The composition of $W_{1-x}Mo_xO_3$ can be readily controlled by varying the ratio of metals in the electrolyte.

The air-dried tungsten–molybdenum mixed oxide films were confirmed to be amorphous as-deposited, and XRD patterns obtained from the library after calcination at 450 °C for 4 h are shown in Fig. 1(a). Several different phases were observed for the mixed oxide films. For example, the XRD pattern of the $W_{0.5}Mo_{0.5}O_3$ film shows three characteristic peaks at 23.3, 25.1, and 26.6°, which clearly distinguish itself from either pure WO_3 or pure MoO_3. Pure tungsten oxide and pure molybdenum oxide exhibit a monoclinic and an orthorhombic α-phase, respectively.[11–13] There is no evidence of superpositional peaks of pure tungsten oxide and pure molybdenum oxide except for the extremely tungsten rich compound ($W_{0.8}Mo_{0.2}O_3$), which indicates that for the most part the mixed oxides ($W_{1-x}Mo_xO_3$) are not simply mixed phases of the two pure oxides.

Raman spectra were obtained by photoexcitation with a 514.5 nm Ar ion laser (Spectra Physics). Raman scattering signals were collected in a back-scattering geometry using a thermoelectrically cooled CCD detector (Jobin-Yvon/ISA Spectrum One). Raman spectra of selected library members are shown in Fig. 1(b). For pure tungsten oxide, two broad peaks were observed at 715 and 807 cm^{-1}, which are characteristic of the corner-shared oxygen (W–O–W) of the monoclinic WO_3 structure.[14] Pure molybdenum oxide shows three characteristic peaks of the α-phase at 668, 821 and 997 cm^{-1}, which represent edge-shared oxygen (Mo_3–O), corner-shared oxygen (Mo–O–Mo), and terminal oxygen (Mo=O), respectively.[15] As the composition of $W_{1-x}Mo_xO_3$ varies, systematic spectral changes are observed. Three bands at 765, 844 and 901 cm^{-1} are observed in the Raman spectrum of $W_{0.5}Mo_{0.5}O_3$; none of which is found in either pure tungsten oxide or pure molybdenum oxide. These bands are consistent with those of β-phase-MoO_3, which has two characteristic peaks at 776 and 850 cm^{-1} as well as a small shoulder at around 900 cm^{-1},[12,13] These bands were shifted

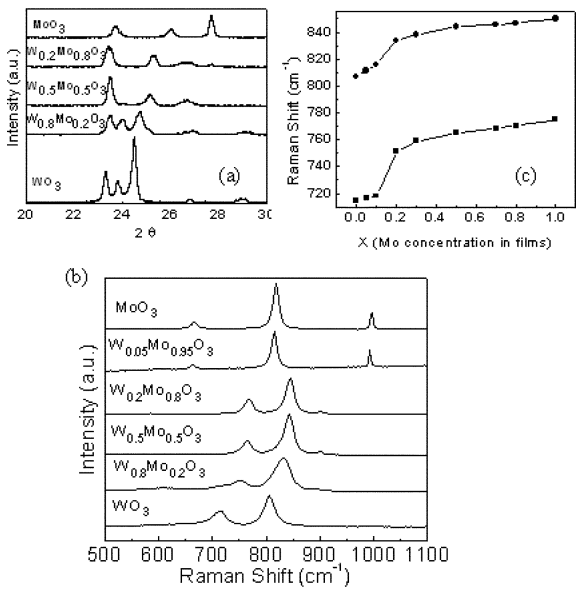

Fig. 1 (a) X-Ray diffraction patterns and (b) Raman spectroscopy of tungsten–molybdenum mixed oxides with respect to film compositions. (c) Raman shift with respect to film compositions. The values at x = 1.0 are from ref. 12. When $0 \leq x \leq 0.9$, monoclinic phase was dominant, but when $x > 0.9$, the α-phase was dominant.

DOI: 10.1039/b313924g

to lower frequency, compared to β-phase-MoO_3. Interestingly, when the molybdenum concentration (x) is less than or equal to 0.9, a monoclinic phase was clearly observed. Above 0.9, a distinct phase transformation had taken place from monoclinic to orthorhombic (α phase). The bandwidths of the new Raman peaks become gradually narrower (by ~50%) with an increase in molybdenum composition, which reveals a significant increase in structural homogeneity. The abrupt structural change at approximately $x = 0.9$ is consistent with the results of Purans *et al*.[16,17] To confirm the lattice structure, we compared the Raman bands of all monoclinic phase mixed oxides with pure β-phase-MoO_3, Fig. 1(c) shows the frequency shifts of the Raman bands with respect to film composition. With increasing molybdenum concentration (x) from 0.2 to 0.8, the positions of the Raman bands of $W_{1-x}Mo_xO_3$ asymptotically approach those of pure β-MoO_3, which supports the notion of $W_{1-x}Mo_xO_3$ as having the β-MoO_3 structure. Although the fundamental β-phase structure is maintained in this composition region, the W-doping results in moderate structural changes and greater crystallographic disorder, as observed by broader Raman bands compared to pure β-MoO_3. A large shift in the Raman spectrum between pure WO_3 and $W_{0.8}Mo_{0.2}O_3$ is evidence of a substantial structural change, implying a transition from monoclinic WO_3 to the β-phase monoclinic MoO_3 structure, despite the fact that the material is W-rich. We summarize the structural change with composition in Table 1. This finding is consistent with the XRD results which showed no evidence of phase separation of either pure tungsten oxide or pure molybdenum oxide.

We investigated the photocatalytic activity of the tungsten–molybdenum mixed oxide library after calcination at 450 °C. Current measurement was obtained while the sample was illuminated with a chopped Xe light source (Oriel) with a light intensity of 25 mW cm^{-2}. A trend in photoresponse as a function of molybdenum composition was clearly observed, Fig. 2(a).

The values of zerobias photocurrent for pure tungsten oxide and molybdenum oxide are 12.3 and 5.9 μA cm^{-2}, respectively. All the films showed n-type semiconducting behavior and the maximum photoresponse was observed for $W_{0.5}Mo_{0.5}O_3$ with photoactivity decreasing as film composition approached either pure oxide. The photoresponse of the $W_{0.5}Mo_{0.5}O_3$ mixed oxide film, 18.5 μA cm^{-2}, was 50% higher than that of the pure tungsten oxide film.

Table 1 Structural change of $W_{1-x}Mo_xO_3$ with respect to film composition (x)

$0 \leq x < 0.2$	Similar to monoclinic WO_3
$0.2 \leq x \leq 0.9$	Similar to monoclinic β-MoO_3
$0.9 < x \leq 1$	Similar to orthorhombic α-MoO_3

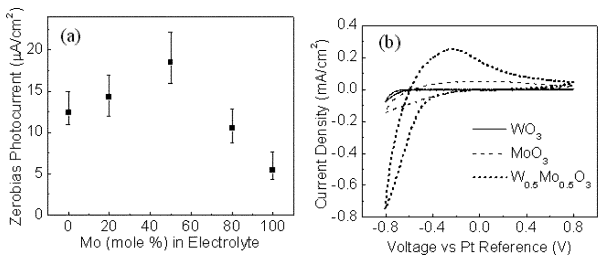

Fig. 2 (a) Zero bias photocurrent of tungsten–molybdenum mixed metal oxide films in 0.1 M sodium acetate. All samples were n-type semiconductors. Illumination was provided by a 150 W Xe lamp. (b) Cyclic voltammograms for potassium intercalation/deintercalation of WO_3 (solid line), MoO_3 (dashed line) and $W_{0.5}Mo_{0.5}O_3$ (dotted line); 0.1 M KCl was used as electrolyte. The scan rate was 100 mV s^{-1}.

Cation intercalations were carried out for the as-synthesized tungsten–molybdenum mixed oxide library using H^+, Li^+, Na^+ and K^+. The electrochromic process of metal oxides has been explained by the double intercalation of a proton and an electron to form a colored metal bronze.[2] The cyclic voltammograms measured for tungsten–molybdenum mixed oxides during potassium (K^+) intercalation are shown in Fig. 2(b). The integrated cathodic current density is a measure of the intercalation capacity. Interestingly, as the ratio of tungsten to molybdenum approaches unity, electrochromic properties improve. Compared to either pure tungsten oxide or pure molybdenum oxide, the mixed oxides show considerably enhanced intercalation properties, with the $W_{0.5}Mo_{0.5}O_3$ film exhibiting the highest intercalation properties of all. All cations (H^+, Li^+, Na^+) revealed the same trend as K^+ (data not shown). We are currently investigating the specific mechanism for photocatalytic and electrochromic improvements in these mixed oxide materials. Previous work has attributed such improvements to the six major ionic species (W^{6+}, W^{5+}, W^{4+}, Mo^{6+}, Mo^{5+}, Mo^{4+}) present in the mixed oxide, which allow for increased inter- and intra-valency charge transfer.[6] Presumably, lattice geometry plays an important role which will be investigated in future work.

Major funding was supported by the Hydrogen Program of the Department of Energy (DOE, Grant # DER-FC36-01G011092). Partial funding and facilities were provided by the NSF-MRSEC funded Materials Research Laboratory (Award # DMR00-80034). T. F. J. would like thank Rockwell Corp. for a Fellowship in Inorganic Materials.

Notes and references

1 J. N. Yao, D. Chen and A. Fujishima, *J. Electroanal. Chem.*, 1996, **406**, 223.
2 C. G. Granqvist, *Sol. Energy Mater. Sol. Cells*, 2000, **60**, 201.
3 M. G. Hutchins, N. A. Kamel, W. El-Kardy, A. A. Ramadan and K. Abdel-Hady, *Phys. Status Solidi A*, 1999, **175**, 991.
4 E. Salje and R. Gehlig, *J. Solid State Chem.*, 1978, **25**, 239.
5 E. E. Khawaja, S. M. A. Durrani and M. A. Daous, *J. Phys.: Condens. Matter*, 1997, **9**, 9381.
6 K. Geshva, A. Szekeres and T. Ivanova, *Sol. Energy Mater Sol. Cells*, 2003, **76**, 563.
7 Z. Cao and J. R. Owen, *Thin Solid Films*, 1995, **271**, 69.
8 P. M. S. Monk, T. Ali and R. D. Partridge, *Solid State Ionics*, 1995, **80**, 75.
9 A. Pennisi, F. Simone and C. M. Lampert, *Sol. Energy Mater. Sol. Cells*, 1992, **28**, 233.
10 S. H. Baeck, K.-S. Choi, A. Ivanovskaya, T. F. Jaramillo, G. D. Stucky and E. W. McFarland, *Proc. 2002, DOE Hydrogen Program Review*, 2002NREL/CP-610-32405.
11 E. Ozkan, S.-H. Lee, P. Liu, C. E. Tracy, F. Z. Tepehan, J. R. Pitts and S. K. Deb, *Solid State Ionics*, 2002, **149**, 139.
12 T. M. McEvoy and K. J. Stevenson, *Langmuir*, 2003, **19**, 4316.
13 M. Figlarz, *Prog. Solid State Films*, 1989, **19**, 1.
14 E. Haro-Poniatowski, M. Jouanne, J. F. Morhange, C. Julien, R. Diamant, M. Fernandez-Guasti, G. A. Fuentes and J. C. Alonso, *Appl. Surf. Sci.*, 1998, **127–129**, 674.
15 S.-H. Lee, M. J. Seong, C. E. Tracy, A. Mascarenhas, J. R. Pitts and S. K. Deb, *Solid State Ionics*, 2002, **147**, 129.
16 A. Kuzmin and J. Purans, *J. Phys.: Condens. Matter*, 2000, **12**, 1959.
17 J. Purans, A. Kuzmin, P. Parent and H. Dexpert, *Physica B*, 1995, **209**, 373.